International Journal of the Korean Society of Precision Engineering, Vol 1, No. 2, December 2000.

Self-Calibration of High Frequency Errors of Test Optics by Arbitrary N-step Rotation

Seung-Woo Kim* and Hyug-Gyo Rhee*

* Department of Mechanical Engineering Science, Korea Advanced Institute of Science and Technology, Taejon, South Korea

ABSTRACT

We propose an extended version of multi-step algorithm of self-calibration of interferometric optical testing instruments. The key idea is to take wavefront measurements with near equal steps in that a slight angular offset is intentionally provided in part rotation. This generalized algorithm adopts least squares technique to determine the true azimuthal positions of part rotation and consequently eliminates calibration errors caused by rotation inaccuracy. In addition, the required number of part rotation is greatly reduced when higher order spatial frequency terms are of particular importance.

Keywords : Optical testing, interferometers, absolute test, self-calibration, Zernike polynomials, least squares

1. Introduction

Self-calibration in optical testing aims to remove the systematic errors of the instrument without relying upon externally calibrated artifacts. This approach of absolute test becomes important when no calibration standards with sufficiently quantified accuracy are available because the required uncertainty in the measurement is of the same order as the instrument errors. Ever since the reversal principle of three-flat test giving one line profile from three setups was first known, a body of practical techniques has been evolved for absolute test of flats and spherical surfaces [1-3]. The majority of work has attempted to obtain complete full aperture solutions in the Twyman-Green and Fizeau interferometers by extending the classical three-flat test. Examples are the so-called cat's eye test [4-7], three-sphericity test [8], transparent three-flat test [9-11], and skip-flat or Ritchey-Common test [12,13]. The cat's eye test works with only three setups elaborately configured for spherical surfaces having an externally accessible focus. The other tests rotate one of the parts stepping out the line measurement principle of the three-flat test over full aperture area. There was another approach of adopting well-defined model functions such as the Zernike polynomials or Fourier series to approximate surface errors [14-19]. The use of model functions offers a general way of removing systematic errors with a minimum number of part rotations, being particularly useful when lower-order errors of spherical, coma and astigmatism aberrations are of primary interest. It also permits improving calibration accuracy through simple arithmetic averaging of measured wavefronts [20-23].

Our discussion in this paper particularly concerns the multi-step averaging method proposed by Evans and Kestner [20]. The underlying principle is averaging multiple wavefronts sampled while rotating the part to N equally spaced azimuthal positions about the optical axis to identify rotationally variant asymmetric wavefront errors. This method works well with only four or six consecutive part rotations in practice, but has a drawback of failing to provide a complete solution since the rotationally invariant and rotationally harmonic wavefront components are not recognizable by part rotation. If higher-order wavefront irregularities are required for rigorous inspection of the part, the number of part rotations should consequently be increased to reduce the partial loss of the rotationally unrecognizable wavefront errors. However, when a large number of part

rotations is implemented, a high precision is required in part rotation because higher order wavefront components are particularly sensitive to rotation errors. This problem could diminish with aids of an accurate azimuthal angle division device, but a more effective way would be improving the current algorithm not to be confined by the equal spacing requirement. Motivated by this, we propose an extended version of the multi-step averaging algorithm, which permits part rotation to be made at arbitrary azimuthal positions. This generalized algorithm eliminates calibration errors caused by rotation inaccuracy and also offers a great advantage of reducing the required number of part rotations when higher order spatial frequency terms are of particular importance. The latter benefit is obtained by imposing a small amount of intentional offset in the azimuthal positions during part rotation.

2. Multi-step Averaging

The resulting wavefront W from any interferometric optical testing is composed of two partial wavefront components of

$$W = T + P \tag{1}$$

where T is the systematic error of the instrument including the reference surface, while P is the surface of the part to be measured. The above simple linear superposition of the two wavefronts is not strictly true but generally valid if they are of small orders as usual in most cases of optical shop testing. To separate the two wavefronts from each other, P is rotated about the optical axis by some physical means while T remains stationary. Then, let W_j be the wavefront of W sampled when P is stationed at an azimuthal position of α_j . The subscript j indicates the rotation index ranging from 0 to N-1, where $\alpha_0 = 0$ and N is the total number of part rotations. T undergoing no changes vanishes in the difference wavefront D_j . which is intermediately defined as the subtraction of

$$D_j = W_j - W_0 = (T + P_j) - (T + P_0) = P_j - P_0 . \tag{2}$$

Now, with the intention of reconstruct P_0 from D_j , the expression of Zernike polynomials is adopted to decompose P_0 such as

$$P_0 = P(r,\theta) = \sum_{l,k} R_l^k(r)[c_{lk}\cos(k\theta) + d_{lk}\sin(k\theta)] \tag{3}$$

where r and θ are the normalized radial and angular coordinates; Rkl(r) the radial polynomials; clk and dlk the coefficients of the angular terms. In line with P0 expressed in Equation (3), the rotated wavefront Pj is also described as

$$\begin{aligned} P_j &= P(r,\theta+\alpha_j) \\ &= \sum_{l,k} R_l^k(r)[c_{lk}\cos(k\theta+\alpha_j) + d_{lk}\sin(k\theta+\alpha_j)] \\ &= \sum_{l,k} R_l^k(r)[c_{lk}'\cos(k\theta) + d_{lk}'\sin(k\theta)] \end{aligned} \tag{4}$$

where $c_{lk}' = c_{lk}\cos(k\alpha_j) + d_{lk}\sin(k\alpha_j)$
and $d_{lk}' = d_{lk}\cos(k\alpha_j) - c_{lk}\sin(k\alpha_j)$.

Equations (3) and (4) indicate that the Zernike coefficients c_{lk} and d_{lk} comply with the well-known transformation rule of vector rotation when they are regarded as the two orthogonal magnitude components of a two-dimensional vector. Then, substituting both the Zernike expressions of P_0 and P_j into Equation (2) allows the coefficients of the difference wavefront D_j to be obtained such as $\Delta c_{lk} \equiv c_{lk} - c_{lk}'$ and $\Delta d_{lk} \equiv d_{lk} - d_{lk}'$. Therefore, once D_j have actually been sampled and fitted to solve for Δc_{lk} and Δd_{lk}, the coefficients of the original part wavefront P_0 are readily determined as

$$c_{lk} = \frac{1}{2}\left[\Delta c_{lk} + \frac{\Delta d_{lk}\sin(k\alpha_j)}{(1-\cos(k\alpha_j))}\right],$$

$$\text{and } d_{lk} = \frac{1}{2}\left[\Delta d_{lk} - \frac{\Delta c_{lk}\sin(k\alpha_j)}{(1-\cos(k\alpha_j))}\right]. \tag{5}$$

In fact, this result was first proposed by Parks [14] and Fritz [16]. This is hereafter referred to as the two-step algorithm as it is capable of providing a solution with only two measurements of wavefronts, i.e., j=0 and

1. The algorithm is convenient to implement with merely one part rotation of P, but the solution is not complete since the denominator 1-cos(kα) becomes null for certain angular orders of k. One case for the void situation is when k=0, implying that all the rotationally invariant components of P0 are not recovered. The other includes all the cases when k is integer multiples of $2\pi/\alpha$, which means that even rotationally harmonic components are partially lost. It is theoretically desirable to take the rotation angle as small as possible to increase the least integer multiple of $2\pi/\alpha$, but too small α tends to provoke computational inaccuracy especially for lower orders of k [21].

Now we proceed to the multi-step algorithm that takes multiple part rotations to give the arithmetic mean of the measured wavefronts as the solution. To explain its underlying principles, by substituting Equations (3) and (4) into Equation (2), the difference wavefront is rearranged in the form of

$$D_j = P_0[\cos(k\alpha_j) - 1] + \widetilde{P}_0 \sin(k\alpha_j) \tag{6}$$

where $\widetilde{P}_0$ is a conjugate wavefront of P_0, i.e.,

$$\widetilde{P}_0 = \sum_{l,l} R_l^k(r)[d_{lk} \cos(k\theta) - c_{lk} \sin(k\theta)] .$$

Then, summing up all the difference wavefronts leads to the expression of

$$\sum_{j=0}^{N-1} D_j = P_0[\sum_{j=0}^{N-1} \cos(k\alpha_j) - N] + \widetilde{P}_0 \sum_{j=0}^{N-1} \sin(k\alpha_j) . \tag{7}$$

The key idea of the multi-step algorithm is to take the azimuthal angles to be equally spaced such as $\alpha_j = 2\pi j/(N\text{-}1)$, with the intention of making the most of the invariant properties of the sine and cosine harmonic functions of

$$\sum_{j=0}^{N-1} \sin(k\alpha_j) = 0 \text{ for all } k, \text{ and} \tag{8}$$

$$\sum_{j=0}^{N-1} \cos(k\alpha_j) = 0 \text{ for k not being integer multiples of N, otherwise } \sum_{j=0}^{N-1} \cos(k\alpha_j) = N. \tag{9}$$

Thus, if both the sums of sine and cosine terms are zero, Equation (7) leads to the final form of the multi-step algorithm of

$$P_0 = \frac{1}{N} \sum_{j=0}^{N-1} D_j . \tag{10}$$

This result was first proposed by Evans and Kestner [20], and named the multi-step averaging algorithm. In comparison with the previous two-step algorithm, this arithmetic algorithm requires less computation since the Zernike fit of D_j is not necessary. Further, averaging of multiple wavefronts improves calibration accuracy because any sampling error in a single wavefront is averaged out However, the problem of partial wavefront loss still remains; the rotationally invariant components of k=0 as well as the rotationally harmonic components of k being integer multiples of N are not recovered as implied in Equation (9). For general optical testing when low-order spherical, coma and astigmatism aberrations are of interest, four or six part rotations are usually sufficient [20, 22]. When higher-frequency wavefront irregularities of the part are to be rigorously examined, N should be increased with a large number of subsequent wavefront measurements. The number of part rotations may be reduced by adapting the software rotation technique [23], which takes only two actual wavefronts with part rotation and then synthetically generates other wavefronts by transforming the two real wavefronts in consideration of rotation geometry. In this case, however, any sampling errors encountered in the two measured wavefronts due to rotation inaccuracy and electrical noise significantly deteriorate the final calibration results with no averaging effects. More practical way of reducing the number of part rotations while maintaining averaging effects may be to split N into two numbers such as $N = N_1 \cdot N_2$. Then two separate sequences of multi-step averaging measurements are performed; one with N_1 rotations and the other with N_2 rotations. If N_1 and N_2 are incommensurate, the errors in the test part can be determined up to the order of N_1 times N_2 by fitting the measurement results to Zernike polynomials. For

example, if N is required to be 72 for an angular bandwidth of 5°. N_1 and N_2 are determined as 8 and 9 respectively. This consequently reduces the total number of rotations from 72 to 17.

3. Least Squares Algorithm

If one adopts the well known shifting theorem of Fourier transform, it becomes clear that partial wavefront loss is unavoidable in both the two-step and multi-step averaging algorithms. The difference wavefront of Equation (2) is transformed into the spectral domain of the angular coordinate such as

$$\begin{aligned}\Im\{D_j\} &= \Im\{P(\theta+\alpha_j)-P(\theta)\} \\ &= \Im\{P(\theta)\}\cdot\{\exp[-ik\alpha_j]-1\}\end{aligned} \tag{11}$$

The notion $\Im\{\cdot\}$ represents the Fourier transform. The part wavefront $P(\theta)$ is then obtained as

$$P(\theta) = \Im^{-1}\left\{\frac{1}{\{\exp[-ik\alpha_j]-1\}}\Im\{D_j\}\right\} \tag{12}$$

where $\Im^{-1}$ represents the inverse Fourier transform. If $k\alpha_j = 2\pi n$ for $n = 0,1,2, \ldots$ the above equation is no longer valid since the denominator of the right hand side becomes null, i.e.,

$$\exp[-i2\pi n]-1 = \{\cos 2\pi n - \sin 2\pi n\}-1 = \{0-1\}-1 = 0$$

This exactly corresponds to the void situations of the two-step algorithm, in which all the angular orders of $k = 2\pi n/\alpha_j$ are lost. Similar discussions apply to the multi-step averaging algorithm, for which the part wavefront $P(\theta)$ is derived as

$$P(\theta) = \Im^{-1}\left\{\frac{1}{\{\sum_{j=0}^{N-1}\exp[-ik\alpha_j]-N\}}\Im\{\sum_{j=0}^{N-1}D_j\}\right\}. \tag{13}$$

In this case, if k is either zero or integer multiples of N, the solution of $P(\theta)$ is not determined since the denominator becomes null. This is readily verified by utilizing the invariant properties of sine and cosine harmonic functions explained in Equations (8) and (9) such as

$$\begin{aligned}&\sum_{j=0}^{N-1}\exp[-ik\alpha_j]-N \\ &= \sum_{j=0}^{N-1}\cos k\alpha_j - \sum_{j=0}^{N-1}\sin k\alpha_j - N. \\ &= N-0-N=0\end{aligned}$$

From the above discussions, it may be deduced that one way of avoiding the void situations in the multi-step method is to select the rotation angles α_j deliberately not to be equally spaced so that the void condition of the denominator is weakened. This approach provides another advantage of reducing the total number of part rotation can be reduced for a given angular bandwidth of measurement. For example, it was explained in the previous section that a total of 17 part rotations are required for an angular bandwidth of 5°. The same calibration results are produced with only six measurements if α_j are chosen as 0°, 65°, 125°, 175°, 245°, and 295°, where an offset of 5° is intentionally added or subtracted respectively to the six equally spaced angles around one revolution. In modifying the current multi-step averaging algorithm not to be confined by the equal spacing requirement, it is necessary to identify the true values of α_j directly from measured wavefronts. The reason is that in performing the multi-step algorithm, many practical difficulties arise in maintaining a high precision in part rotation especially when a large number of rotations are required with an intentional offset. Consequently, the key idea of the newly proposed algorithm is that the rotated angles α_j are treated as additional unknowns together with the coefficients c_{lk} and d_{lk}. Then their actual values are determined from the measured wavefronts D_j using least-squares technique.

The new multi-step algorithm beings with decomposing the part wavefront in terms of the angular

order is k such as $P(r,\theta)=\sum_{k} P^k(r,\theta)$, where $P^k(r,\theta)$ is the partial sum of all the Zernike radial polynomial components whose angular order is k. Letting $L(k)$ be the maximum radial order to be considered for each k, the partial sum is made up in detail such as

$$P^k(r,\theta)=\sum_{l}^{L(k)} R_l^k(r)[c_{lk}\cos(k\theta)+d_{lk}\sin(k\theta)] =\sum_{l}^{L(k)}\xi_l^k Z_l^k(r,\theta) \tag{14}$$

where $Z_l^k(r,\theta)\equiv R_l^k(r)\begin{Bmatrix}\cos\\ \sin\end{Bmatrix}(k\theta)$ and ξ_l^k denotes another form of Zernike coefficients. Similarly, the sampled wavefront difference D_j is also expressed as $D_j(r,\theta)=\sum_{k=1}^{K} D_j^k(r,\theta)$ in which

$$\begin{aligned} &D_j^k(r,\theta)\\ &=P_0^k(r,\theta)[\cos(k\alpha_j)-1]+\tilde{P}_0^k(r,\theta)\sin(k\alpha_j)\\ &=\sum_{l}^{L(k)}\{\xi_{0l}^k Z_l^k(r,\theta)[\cos(k\alpha_j)-1]+\tilde{\xi}_{0l}^k Z_l^k(r,\theta)\sin(k\alpha_j)\}\\ &\equiv\sum_{l}^{L(k)} X_{lj}^k Z_l^k(r,\theta) \end{aligned} \tag{15}$$

For convenience, the subscript i is newly introduced to replace the notation (r,θ) such as $D_{ij}^k=\sum_{l}^{L(k)} X_{lj}^k Z_{li}^k$.

Now, let $\hat{D}_{ij}^k$ be the actually measured value of D_{ij}^k. Then computation for Zernike fitting of $\hat{D}_{ij}^k$ and subsequent partial summing of the coefficients with same order of k allows X_{lj}^k of Equation (15) to be computed as $\hat{X}_{lj}^k$. In doing that, if the values of α_j are not correctly estimated, the computed values of $\hat{X}_{lj}^k$ never equal the true values of X_{ij}^k . The computational errors in $\hat{X}_{lj}^k$ are arranged in the form of two cost functions, which are defined for each k such as

$$\begin{aligned} E_l^k&=\sum_{j=0}^{N-1}\{X_{lj}^k-\hat{X}_{lj}^k\}^2\\ &=\sum_{j=0}^{N-1}\left\{\xi_{0l}^k[\cos(k\alpha_j)-1]+\tilde{\xi}_{0l}^k\sin(k\alpha_j)-\hat{X}_{lj}^k\right\}^2 \end{aligned} \tag{16}$$

and

$$\begin{aligned} E_j^k&=\sum_{l}^{L(k)}\{X_{lj}^k-\hat{X}_{lj}^k\}^2\\ &=\sum_{l}^{L(k)}\left\{\xi_{0l}^k[\cos(k\alpha_j)-1]+\tilde{\xi}_{0l}^k\sin(k\alpha_j)-\hat{X}_{lj}^k\right\}^2 \end{aligned} \tag{17}$$

The former E_l^k represents the partial error sum of induced in the radial coefficients of Zernike fitting by inaccurate estimation of rotation angles α_j . On the other hand, the latter E_j^k is the partial sum of errors resulting in the j-th wavefront. The cost functions should be minimized to determine the true values of the unknowns of ξ_{0l}^k , $\tilde{\xi}_{0l}^k$ and α_j . The necessary conditions are derived as

$$\frac{\partial E_l^k}{\partial\xi_{0l}^k}=\frac{\partial E_l^k}{\partial\tilde{\xi}_{0l}^k}=\frac{\partial E_j^k}{\partial\cos(k\alpha_j)}=\frac{\partial E_j^k}{\partial\sin(k\alpha_j)}=0. \tag{18}$$

The above conditions are arranged in the form of matrix equations such as

$$\begin{bmatrix} \sum_{j=0}^{N-1}[\cos(k\alpha_j)-1]^2 & \sum_{j=0}^{N-1}\sin(k\alpha_j)[\cos(k\alpha_j)-1]\\ \sum_{j=0}^{N-1}\sin(k\alpha_j)[\cos(k\alpha_j)-1] & \sum_{j=0}^{N-1}\sin^2(k\alpha_j)\end{bmatrix}\begin{bmatrix}\xi_{0l}^k\\ \tilde{\xi}_{0l}^k\end{bmatrix} =\begin{bmatrix}\sum_{j=0}^{N-1}\hat{X}_{lj}^k[\cos(k\alpha_j)-1]\\ \sum_{j=0}^{N-1}\hat{X}_{lj}^k\sin(k\alpha_j)\end{bmatrix} \tag{19}$$

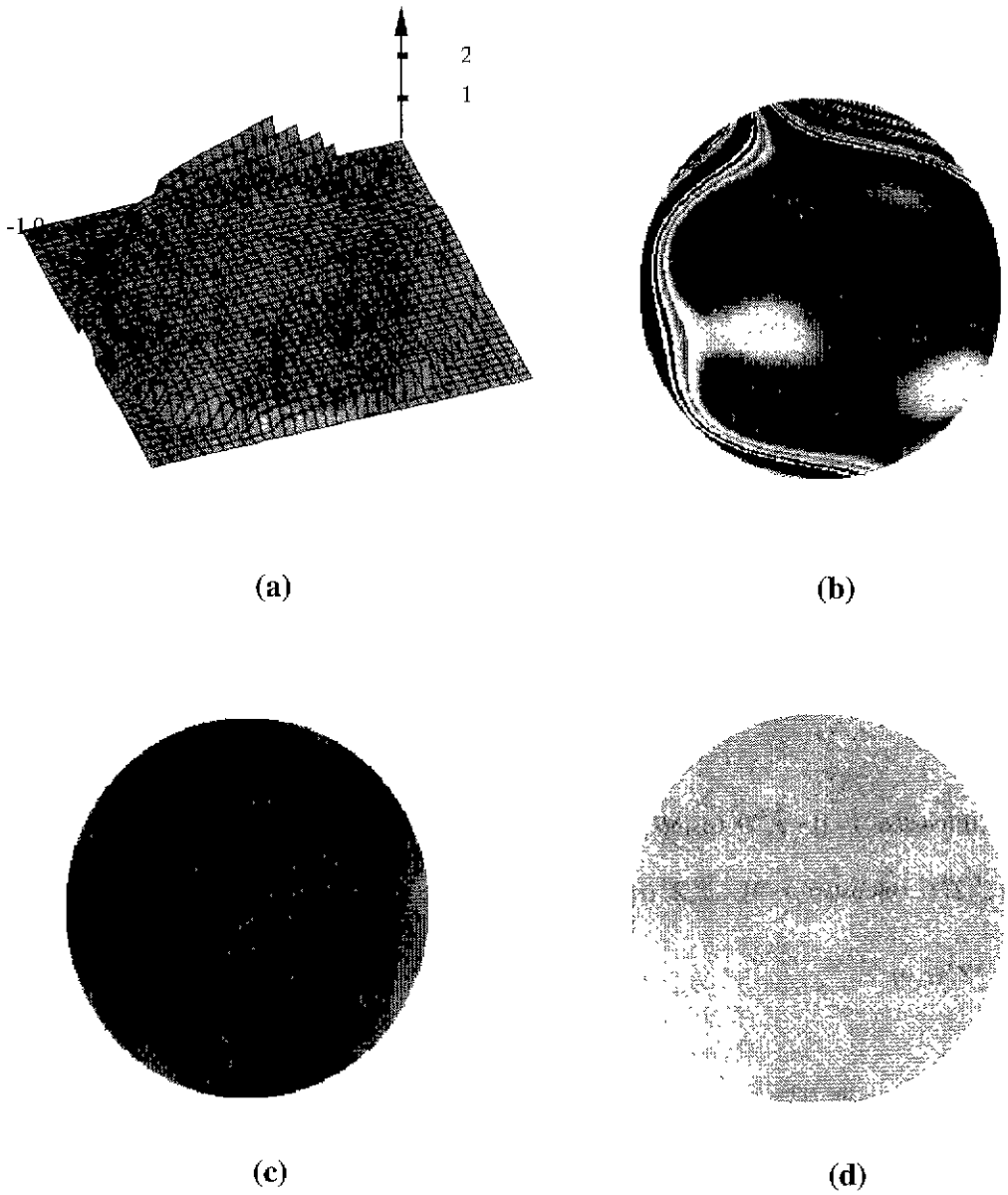

Fig. 1 Comparison of simulation results when true values of α_j are not equally spaced mistakenly as 0°, 61°, 121°, 179°, 241°, 299°. (a) Original wavefront generated for simulation with all the Zernike coefficients being 0.1λ for k=1-5. (b) Fringe map of the original wavefront (P-V: 1.118μm and rms: 0.110λ). (c) The wavefront error extracted by the 6-step averaging algorithm (P-V: 0.017μm and rms: 0.001λ). (d) The wavefront error computed by the least-squares algorithm (P-V: 0.001μm and rms value. $3x10^{-7}$λ).

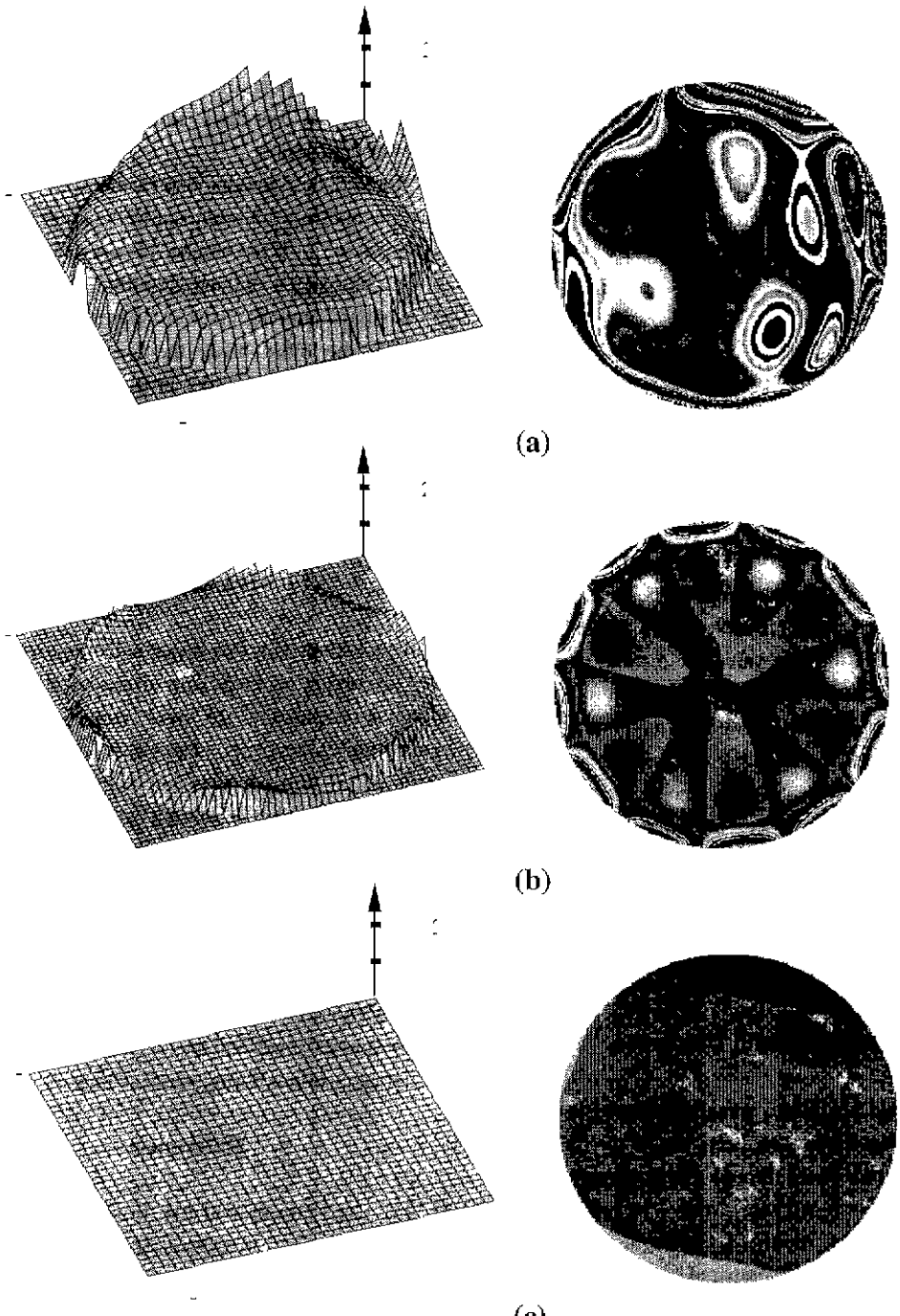

Fig. 2 Suppression capabilities of high frequency components when α_i are intentionally taken as 0°, 61°, 121°, 179°, 241°, 299° (a) Original wavefront generated for simulation with all the Zernike coefficients being 0.1λ for k=1-8 (P-V: 1.763μm and rms: 0.110λ). (b) The wavefront error extracted by the 6-step averaging algorithm (P-V: 0.409μm and rms: 0.001λ). (c) The wavefront error computed by the least-squares algorithm (P-V: 0.012μm and rms value: $2\times10^{-5}\lambda$).

$$\begin{bmatrix} \sum_{l}^{L(k)} [\xi_{0l}^{k}]^2 & \sum_{l}^{L(k)} \xi_{0l}^{k} \tilde{\xi}_{0l}^{k} \\ \sum_{l}^{L(k)} \xi_{0l}^{k} \tilde{\xi}_{0l}^{k} & \sum_{l}^{L(k)} [\tilde{\xi}_{0l}^{k}]^2 \end{bmatrix} \begin{bmatrix} \cos(k\alpha_j) \\ \sin(k\alpha_j) \end{bmatrix}$$

$$= \begin{bmatrix} \sum_{l}^{L(k)} \{\hat{X}_{lj}^{k} \xi_{0l}^{k} + [\xi_{0l}^{k}]^2\} \\ \sum_{l}^{L(k)} \{\hat{X}_{lj}^{k} \tilde{\xi}_{0l}^{k} + \xi_{0l}^{k} \tilde{\xi}_{0l}^{k}\} \end{bmatrix} \tag{20}$$

No analytical solutions are found for the above simultaneous equations, thus iterative numerical technique is adapted. For each k, an initial guess is made for the azimuthal positions α_j so that ξ_{0l}^{k} and $\tilde{\xi}_{0l}^{k}$ are computed from Equation (19). Then by using computed values of ξ_{0l}^{k} and $\tilde{\xi}_{0l}^{k}$, the azimuthal positions α_j are upgraded from Equation (20). Next step is go back to Equation (19) with the new values of α_j and repeat the computation of ξ_{0l}^{k} and $\tilde{\xi}_{0l}^{k}$, and α_j is adjusted again. The iterative computation between Equations (19) and (20) continues until the change of α_j converges into a predefined small value. Total computation time is influenced by the number of terms of Zernike polynomials in consideration, the number of rotation N, and the initially guess of α_j. Finally, with the converged values of ξ_{0l}^{k}, the part wavefront P_0 is reconstructed.

4. Simulation and Discussion

The proposed algorithm, hereafter referred to as the least squares algorithm, has been tested to verify its advantages and usefulness through computer simulation. Figure 1 describes a case study in which the performances of the multi-step averaging and least squares algorithms are compared when there are significant amounts of azimuthal position errors in part rotations. Figure 1(a) illustrates the instrument error to be eliminated while the part wavefront is assumed perfectly flat. The number of steps was taken as 6 equally for both the algorithms and the maximum Zernike order of interest was k=5. Comparison reveals that the least squares algorithm effectively removes almost all the instrument error although part rotations are not accurately induced as intended. On the other hand, the multi-step averaging algorithm is limited in restoring the part wavefront especially around the circumference of the measured area.

Figure 2 describes another case in which higher order instrument errors are dominant in the range of k = 6 to 8 as shown in (a). If the number of part rotation is taken as 6, the multi-step averaging algorithm fails to remove the 6th angular harmonic error components as illustrated in (b). On the other hand, the least squares algorithm suppresses the higher order instrument errors even with the same number of part rotations, demonstrating that higher order surface irregularities of the part are examined accurately. Detailed numerical data for comparison are listed in the figure.

5. Conclusions

Our intention in this paper is to improve the multi-step averaging method with a particular attention of effective separation of the rotationally harmonic wavefront components. The least squares algorithm proposed in this paper is not confined by the equal spacing requirement, permitting part rotations to be made at arbitrary azimuthal positions. This generalized algorithm eliminates calibration errors caused by rotation inaccuracy and also offers a great advantage of reducing the required number of part rotations drastically when higher order spatial frequency terms are of particular importance. The latter benefit is obtained by imposing a predetermined small amount of intentional offset in the azimuthal positions during part rotations.

References

1. J.E. Greivenkamp and J.H. Bruning, "Phase shifting interferometry," in *Optical Shop Testing*, 2nd ed., D. Malacara, ed., Wiley, New York, Chap.14, 577(1992).
2. C. Evans, R. Hocken, and W. Estler, "Self-calibration: reversal, redundancy, error separation, and absolute testing," Annals of the CIRP 45(2), 617(1996).
3. M.V. Mantravadi, "Newton, Fizeau, and Haidinger interferometers," in *Optical Shop Testing*, 2nd ed., D. Malacara, ed., Wiley, New York, Chap.1. 43(1992).

4. A.E. Jensen, "Absolute calibration method for laser Twyman-Green wave-front testing interferometers," J. Opt. Soc. Am. 63, 1313(1973).
5. J.H. Bruning, D.R. Herriott, J.E. Gallagher, D.P. Rosenfeld, A.D. White, and D.J. Brangaccio, "Digital wavefront measuring interferometer for testing optical surfaces and lenses," Appl. Opt. 13, 2693(1974).
6. B.E. Traux, "Absolute interferometric testing of spherical surfaces," Proc. SPIE 966, 130(1988).
7. K.-E. Elssner, R. Burow, J. Grzanna, and R. Spolaczyk, "Absolute sphericity measurement," Appl. Opt. 28, 4649(1989).
8. L.A. Selberg, "Absolute testing of spherical surfaces,' in *Optical Fabrication and Testing*, OSA 1994 Technical Digest Series, 181(1994).
9. G. Schulz and J. Schwider, "Precision measurement of planeness," Appl. Opt. 6, 1077(1967); "Interferometric testing of smooth surfaces," in *Progress in Optics*, E. Wolf, ed. Pergamon, Oxford, 94(1976).
10. G. Shulz and J. Grzanna, "Absolute flatness testing by the rotation method with optimal measuring error compensation," Appl. Opt. 31(19), 3767(1992).
11. K.-E. Elssner, A. Vogel, J. Grzanna, and G. Shulz, "Establishing a flatness standard," Appl. Opt. 33(13), 2437(1994).
12. K.L. Shu, "Ray-trace analysis and data reduction methods for the Ritchey-Common test," Appl. Opt. 22, 1879(1983).
13. F.M. Kuchel, "Absolute measurement of flat mirrors in the Ritchey-Common test," in *Optical Fabrication and Testing*, OSA 1986 Technical Digest Series, 114(1986).
14. R.E. Parks, "Removal of test optics errors, " Proc. SPIE, 153, 56(1978).
15 K. Creath, J.C. Wyant, "Absolute measurement of surface roughness," Appl. Opt. 29, 3823(1990).
16. B.S. Fritz, "Absolute calibration of an optical flat," Opt. Eng. 23, 379(1984).
17. C. Ai and J.C. Wyant, "Absolute testing of flats decomposed to even and odd functions," in *Interferometry: Surface Characterization and Testing*, K. Creath and J.E. Greivenkamp, eds., Proc. Soc. Photo-Opt. Instrum. Eng. 1776, 73(1992).
18. C. Ai and J.C. Wyant, "Absolute testing of flats using even and odd functions," Appl. Opt. 32, 4698(1993).
19. V. Greco, R. Tronconi, C.D. Vecchio, M. Trivi, and G. Molesini, "Absolute measurement of planarity with Fritz's method: uncertainty evaluation," Appl. Opt. 38(10), 2018(1999).
20. C. Evans, R. Kestner, "Test optics error removal," Appl. Opt. 35(7), 1015(1996).
21. V.B. Gubin, V.N. Sharonov, "Algorithm for reconstructing the shape of optical surfaces from the results of experimental data," Sov. J. Opt. Technol. 57(3), (1990).
22. W.T. Estler, C.J. Evans, L.Z. Shao, "Uncertainty estimation for multi-position form error metrology," Prec. Eng. 21(2/3), 72(1997).
23. R.E. Parks, L. Shao, and C.J. Evans, "Pixel-based absolute topography test for three flats," Appl. Opt. 37(25), 5951(1998).